On the Orientation of Vortical Structures in Rotating and Sheared Homogeneous Turbulence

Frank G. Jacobitz

Department of Mechanical Engineering
University of San Diego
5998 Alcalá Park
San Diego, CA 92110, USA
jacobitz@sandiego.edu

Joylene C. Aguirre

Department of Mechanical Engineering
University of San Diego
5998 Alcalá Park
San Diego, CA 92110, USA
joyleneaguirre@sandiego.edu

Adam F. Moreau

Department of Electrical Engineering
University of San Diego
5998 Alcalá Park
San Diego, CA 92110, USA
adammoreau@sandiego.edu

ABSTRACT

Based on the results of a series of direct numerical simulations, the effect of rotation on the orientation of vortical structures is investigated in homogeneous rotating and sheared turbulence. The ratio of the rotation to shear rate is varied and flows without rotation, with moderate rotation, and with strong rotation are considered. The rotation axis is oriented either in the parallel or anti-parallel direction to the mean flow vorticity. For moderate rotation, the anti-parallel configuration results in an increased growth rate of the turbulent kinetic energy, while the parallel configuration leads to a decreased growth rate as compared to shear flow without rotation. Vortical structures inclined in the vertical direction and to the downstream direction are observed and characterized using the three-dimensional two-point autocorrelation coefficient of vorticity magnitude. An ellipsoid is then fitted to the surface given by a constant autocorrelation coefficient value and the major axis is used to determine the inclination angle of flow structures in the plane of shear. For moderate rotation, the structure inclination angle is observed to reach a maximum value in the anti-parallel configuration and to be reduced in the parallel configuration. The strongly rotating cases result in smaller structure inclination angles, which are almost independent of the flow configuration. Therefore, the structure inclination angle of vortical structures appears to be directly related to the dynamics of the flow.

INTRODUCTION

The results from a series of direct numerical simulations of homogeneous rotating and sheared turbulence are used here to study the orientation of vortical structures present in such flows. Homogeneous rotating and sheared turbulence has been studied extensively in the past due to its occurrence in many geophysical or engineering flows (see for example Miesch (2005)). Bradshaw (1969) and Tritton (1992) found rotation to be destabilizing in the anti-parallel configuration for the rotation to shear rate ratio range $0 < f/S < 1$ and stabilizing otherwise. Based on linear theory, Cambon *et al.* (1994) further investigated rotating and sheared homogeneous turbulence and Salhi & Cambon (1997) pointed out that the Bradshaw number $B = f/S(f/S-1)$ is not sufficient to describe the flow evolution. For example, the cases with $f/S = 0$, corresponding to pure shear, and $f/S = 1$, corresponding to zero absolute vorticity, result in the same Bradshaw number $B = 0$, but their evolution differs.

Comprehensive studies of rotating and sheared homogeneous turbulence include the work by Salhi & Cambon (1997), Brethouwer (2005), and Jacobitz *et al.* (2008, 2010, 2016). These studies cover a wide range of parameter regimes and report on many aspects of the flow. For example, Jacobitz *et al.* (2008) addresses inclined vortical structures present in the flows and Brethouwer (2005) performs an analysis in a reference frame tilted into the direction of the inclined structures. Linear theory has been applied by Salhi (2002) and Kassinos *et al.* (2007) to investigate similarities of the effect of rotation and stratification in turbulent shear flows. Salhi *et al.* (2014) use direct numerical simulations and spectral linear theory to disentangle the linear and nonlinear dynamics of this flow. Homogeneous turbulence dynamics in general are discussed by Sagaut & Cambon (2008).

Structures in wall-bounded turbulent flows have been studied starting with the work by Theodorsen (1952). Examples are stud-

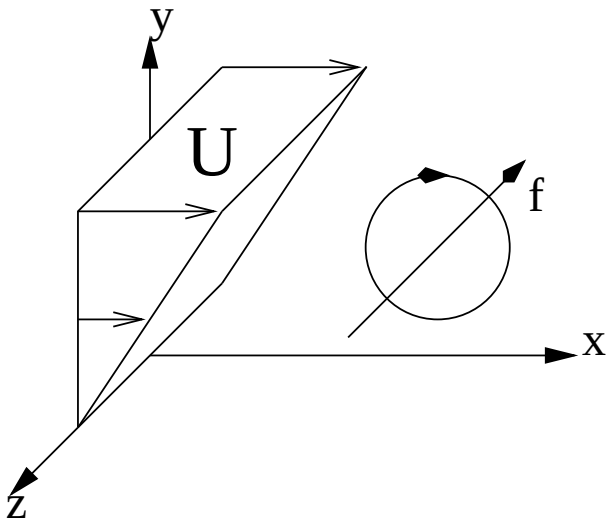

Figure 1. Schematic of flow with uniform shear and system rotation.

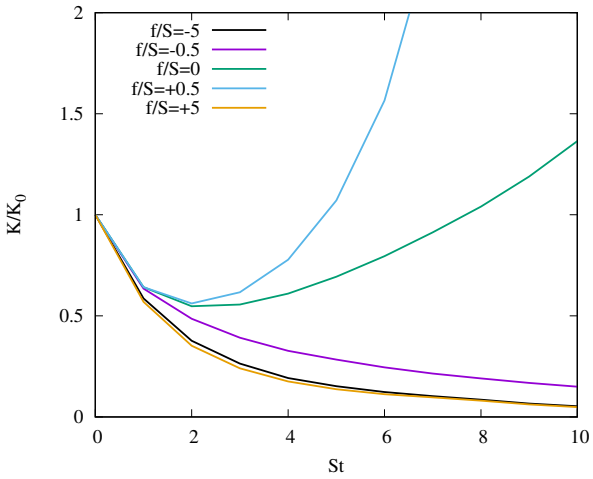

Figure 2. Evolution of the turbulent kinetic energy K in non-dimensional time St for rotation to shear rate ratios ranging from $f/S = -5$ to $f/S = +5$.

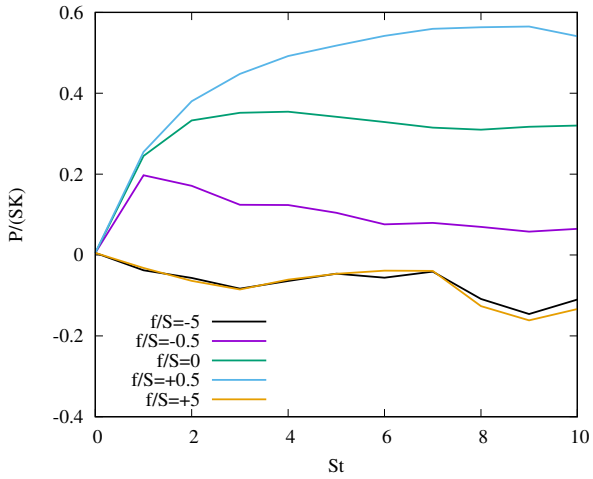

Figure 3. Evolution of the normalized production rate $P/(SK)$ in non-dimensional time St for rotation to shear rate ratios ranging from $f/S = -5$ to $f/S = +5$.

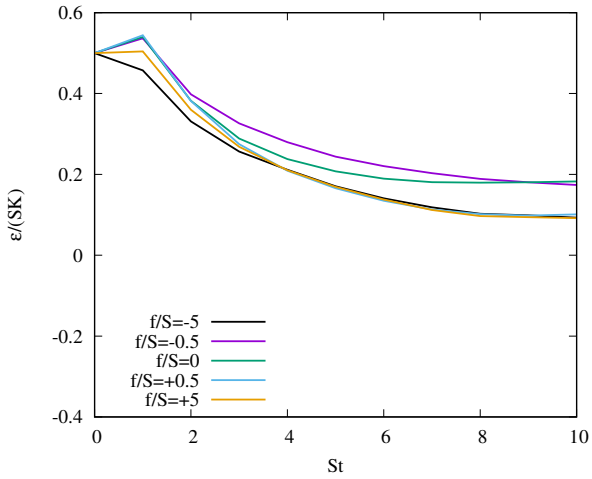

Figure 4. Evolution of the normalized dissipation rate $\varepsilon/(SK)$ in non-dimensional time St for rotation to shear rate ratios ranging from $f/S = -5$ to $f/S = +5$.

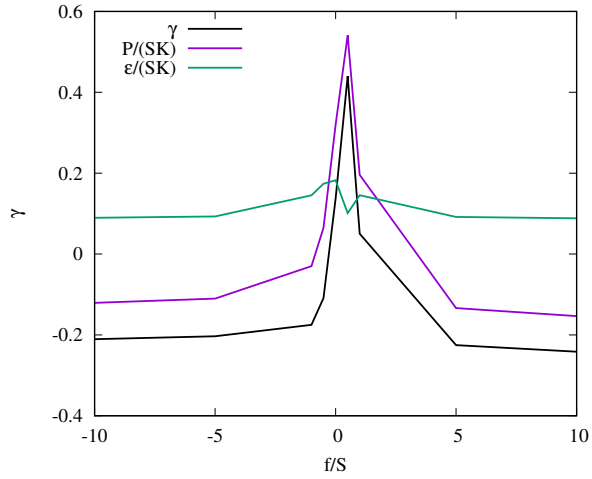

Figure 5. Dependence of the growth rate γ, the normalized production rate $P/(SK)$, and the normalized dissipation rate $\varepsilon/(SK)$ on the rotation to shear rate ratio f/S at non-dimensional time $St = 10$.

ies of streaks (see for example Bakewell & Lumley (1967) or Kim & Lim (2000)) or bursting (see for example Kline *et al.* (1967) or Wallace *et al.* (1972)). More recently, Dong *et al.* (2017) compares structures in homogeneous turbulent shear flows with those in turbulent channel flows. This paper also provides a comprehensive review of work on structures in turbulent flows.

The main aim of this work is a quantitative description of the inclination angle of vortical structures observed in homogeneous rotating and sheared turbulence. In addition, the flow structure, as described by the structure inclination angle, is related to the turbulence dynamics, as described by the growth rate of the turbulent kinetic energy. In the following, the simulation approach is introduced, basic features of the turbulence evolution are recalled, the inclination angle of vortical structures is presented, and conclusions are drawn.

SIMULATION APPROACH

Direct numerical simulations of rotating and sheared homogeneous turbulence are performed in order to quantify the orientation of vortical structures. The flow has vertical shear with constant rate $S = \partial U/\partial y$ and system rotation in the spanwise $z-$direction with constant Coriolis parameter $f = 2\Omega$ (see figure 1). Hence, the system rotation is perpendicular to the plane of shear and either parallel or anti-parallel to the mean flow vorticity. The Cartesian coordinates $\mathbf{x} = (x,y,z) = (x_1,x_2,x_3)$ refer to the streamwise, vertical, and spanwise directions, respectively.

The direct numerical simulations are based on the continuity equation for an incompressible fluid and the unsteady three-dimensional Navier-Stokes equation. The equations of motion for the fluctuating velocities $\mathbf{u} = (u,v,w) = (u_1,u_2,u_3)$ read:

$$\nabla \cdot \mathbf{u} = 0 \tag{1}$$

$$\frac{\partial \mathbf{u}}{\partial t} + \mathbf{u}\cdot\nabla\mathbf{u} + Sy\frac{\partial \mathbf{u}}{\partial x} + Sv\mathbf{e}_x + 2\Omega\times\mathbf{u} = -\frac{1}{\rho_0}\nabla p + \nu\nabla^2\mathbf{u} \tag{2}$$

In these equations, p contains the pressure and the contribution from

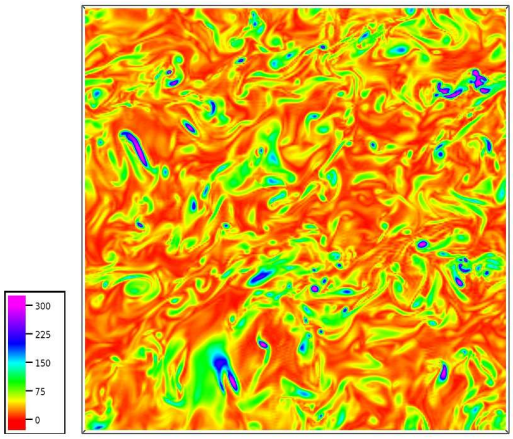

Figure 6. Vorticity magnitude in the plane of shear for a rotation to shear rate ratio $f/S = +0.5$ at non-dimensional time $St = 10$.

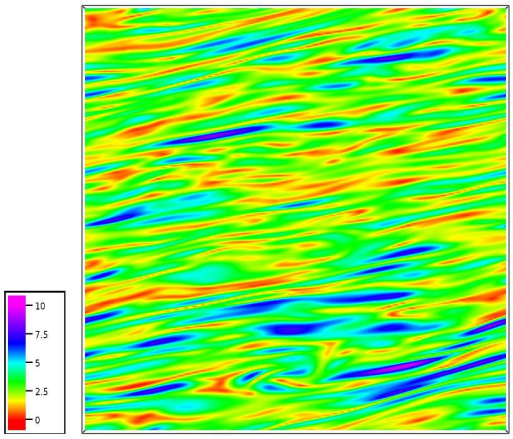

Figure 7. Vorticity magnitude in the plane of shear for a rotation to shear rate ratio $f/S = +0.5$ at non-dimensional time $St = 10$.

the centrifugal force, ρ_0 is the density, ν the kinematic viscosity, and $\mathbf{e}_x$ the unit vector in the downstream direction.

In the direct numerical simulations, all dynamically active scales of the velocity field are resolved. The equations of motion are solved in the Rogallo frame (see Rogallo (1981)) and periodic boundary conditions are used. The spatial discretization is accomplished by a Fourier collocation method and the solution is advanced in time by a fourth-order Runge-Kutta method. The initial conditions are taken from a simulation of decaying isotropic turbulence with an initial Taylor-microscale Reynolds number $Re_\lambda = 56$ and an initial shear number $SK/\varepsilon = 2$. The simulations are performed on a parallel computer using $256 \times 256 \times 256$ grid points.

RESULTS

The results of nine simulations of rotating and sheared homogeneous turbulence are used here to study the orientation of vortical structures in such flows. The rotation to shear rate ratio f/S is varied from -10 to 10. Negative values of f/S correspond to a parallel configuration and positive values correspond to an anti-parallel configuration between the system rotation and the mean flow vorticity (see figure 1).

Flow Evolution

Figure 2 shows the evolution of the turbulent kinetic energy $K = 1/2(u^2 + v^2 + w^2)$ in non-dimensional time St for cases without rotation ($f/S = 0$), with moderate rotation ($f/S = \pm 0.5$), and with strong rotation ($f/S = \pm 5$). After an initial decay due to the isotropic initial conditions, the case without rotation shows eventual exponential growth of the turbulent kinetic energy K. For moderate rotation, the anti-parallel case with $f/S = +0.5$ results in a stronger growth of K as compared to the case without rotation, while the parallel case with $f/S = -0.5$ shows decay of K. For strong rotation with $f/S = \pm 5$, the decay of K is observed to be independent of the flow configuration.

The transport equation for the turbulent kinetic energy K can be written in the following non-dimensional form:

$$\gamma = \frac{1}{SK}\frac{dK}{dt} = \frac{P}{SK} - \frac{\varepsilon}{SK} \tag{3}$$

Here, γ is the growth rate of the turbulent kinetic energy K, $P/(SK)$ the normalized production rate with $P = -S\overline{uv}$, and $\varepsilon/(SK)$ the normalized dissipation rate.

Figures 3 and 4 show the evolution of the normalized production rate $P/(SK)$ and the normalized dissipation rate $\varepsilon/(SK)$, respectively. As a fictitious force, the Coriolis force does not appear in the transport equation for K, but it has a significant effect on the normalized production rate $P/(SK)$. The normalized dissipation rate $\varepsilon/(SK)$, however, remains relatively unaffected by a variation of the rotation to shear rate ratio f/S.

Figure 5 provides a snapshot of the terms in the turbulent kinetic energy transport equation at non-dimensional time $St = 10$. At this time, the different terms have reached an approximately asymptotic value. While the normalized dissipation rate $\varepsilon/(SK)$ remains relatively unaffected by a variation of f/S, the normalized production rate $P/(SK)$ assumes a maximum for $f/S = +0.5$. Similarly, the strongest growth rate γ of the turbulent kinetic energy is observed for $f/S = +0.5$, while the growth rate for $f/S = -0.5$ is less than that for the flow without rotation. For strong rotation, the value of γ is almost unaffected by the flow configuration. More information about the energetics of the flow can be found in Jacobitz *et al.* (2008).

Flow Structures

Figures 6 and 7 show the vorticity magnitude in the plane of shear ($x-y-$plane) at non-dimensional time $St = 10$ for two anti-parallel cases with $f/S = +0.5$, corresponding to moderate rotation and growing turbulent kinetic energy, and with $f/S = +5$, corresponding to strong rotation and decaying turbulent kinetic energy, respectively. Please see Clyne *et al.* (2007) for information about the visualization software. The figures show vortical structures inclined by an angle α in the vertical $y-$direction and to the downstream $x-$direction. The structure inclination angle α is larger for the anti-parallel case with $f/S = +0.5$.

The three-dimensional two-point autocorrelation coefficient of vorticity magnitude is used to quantify the structure inclination angle of the vortical structures:

$$Co_\omega(\mathbf{r}) = \frac{\overline{\omega(\mathbf{x})\omega(\mathbf{x}+\mathbf{r})}}{\omega^2} \tag{4}$$

Here, $\mathbf{r} = (r_x, r_y, r_z)$ is the separation vector. The three-dimensional two-point autocorrelation coefficient of vorticity magnitude is chosen for this analysis, because the autocorrelation is assumed to decrease the slowest in the direction of vorticity magnitude structures

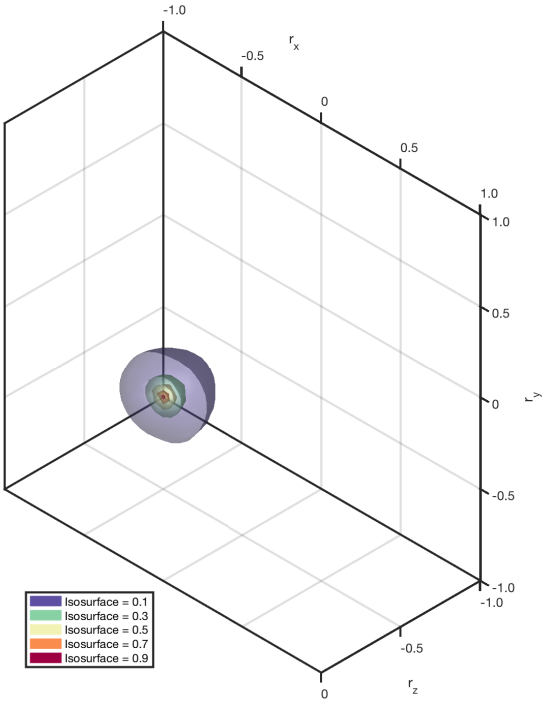

Figure 8. Isosurfaces of the three-dimensional autocorrelation coefficient of vorticity magnitude for a rotation to shear rate ratio $f/S = +0.5$ at non-dimensional time $St = 10$.

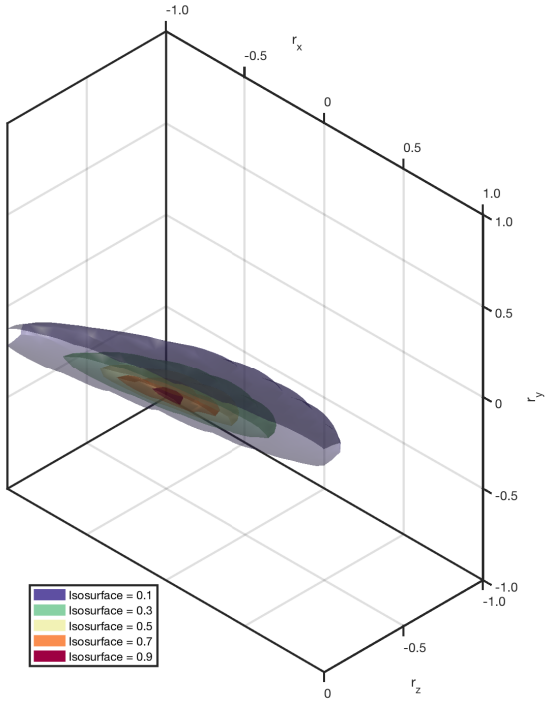

Figure 9. Isosurfaces of the three-dimensional autocorrelation coefficient of vorticity magnitude for a rotation to shear rate ratio $f/S = +5$ at non-dimensional time $St = 10$.

present in the flow.

Figures 8 and 9 show isosurfaces of the two-point autocorrelation coefficient of vorticity magnitude Co_ω at non-dimensional time $St = 10$ for two anti-parallel cases with $f/S = +0.5$ and $f/S = +5$, respectively. The domain is cut in the plane of shear at $r_x = 0$. The isosurfaces form approximately ellipsoid shapes, which grow with decreasing isovalue of Co_ω.

Figures 10 and 11 show the isosurfaces of the three-dimensional two-point autocorrelation coefficient of vorticity magnitude for an autocorrelation coefficient value $Co_\omega = 0.3$ in the plane of shear at non-dimensional time $St = 10$ for two anti-parallel cases with $f/S = +0.5$ and $f/S = +5$, respectively. In addition, an ellipsoid least-square fit to the isosurfaces has been performed. The orientation of the autocorrelation coefficient isosurfaces match the structure inclination angles α of the original vortical structures. The ellipsoid least-square fits very closely match the isosurfaces and the major axes obtained from ellipsoid least-square fits allow for the determination of the structure inclination angles α.

Figures 12 and 13 show the dependence of the structure inclination angle α on the two-point autocorrelation coefficient Co_ω used in its determination at non-dimensional time $St = 10$ for two anti-parallel cases with rotation to shear rate ratios $f/S = +0.5$ and $f/S = +5$, respectively. In both cases, the structure inclination angle value does not change substantially for an interval of autocorrelation coefficients ranging from about $Co_\omega = 0.15$ to $Co_\omega = 0.45$. The figures also indicate the number of isovalues used in the least-squares fit of the ellipsoid. For large autocorrelation coefficient values, only very few points are used to fit the ellipsoid and its orientation is not always well-defined. For small values, the isosurface does not resemble an ellipsoid shape.

Structure and Dynamics

Figure 14 shows the dependence of the structure inclination angle α on the rotation to shear rate ratio f/S. For moderate rotation, the anti-parallel case with $f/S = +0.5$, corresponding to strongly growing turbulent kinetic energy K, results in a structure inclination angle α larger than that observed for the case without rotation ($f/S = 0$), while the parallel case with $f/S = -0.5$, corresponding to decaying K, results in a smaller value of α. For strong rotation, corresponding to strongly decaying K, the lowest values of α are obtained and the values of α are almost independent of the flow configuration. Hence, the dependence of the structure inclination angle α on the rotation to shear rate ratio f/S matches the dependence of the growth rate γ of the turbulent kinetic energy on f/S, shown in figure 5.

Figure 15 shows the dependence of the structure inclination angle α on the growth rate γ. An approximately linear relationship of the two quantities is obtained: Strongly growing cases are characterized by a large structure inclination angle, while decaying cases have a small structure inclination angle. Therefore, it seems that the eventual evolution of rotating and sheared homogeneous turbulence is directly related to the orientation of the vortical structures present in the flow.

The described analysis has been repeated using the magnitude of velocity instead of the magnitude of vorticity and the results are also shown in figures 14 and 15. The structure inclination angles obtained using the velocity magnitude are slightly smaller than those obtained using the vorticity magnitude. The dependence on the rotation to shear rate ratio f/S is maintained. Also, the dependence on the growth rate is also linear, but the relationship appears to have a smaller slope.

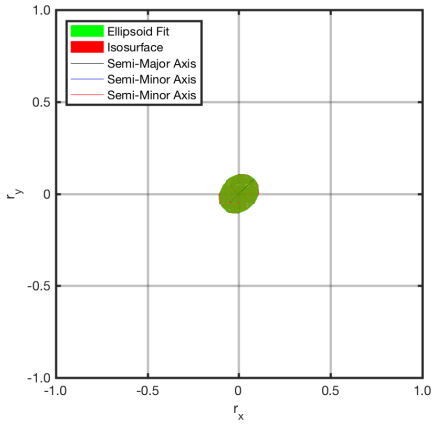

Figure 10. Isosurface and ellipsoid fit of the three-dimensional autocorrelation coefficient of Vorticity magnitude for a value of $Co_\omega = 0.3$ in the plane of shear for a rotation to shear rate ratio $f/S = +0.5$ at non-dimensional time $St = 10$.

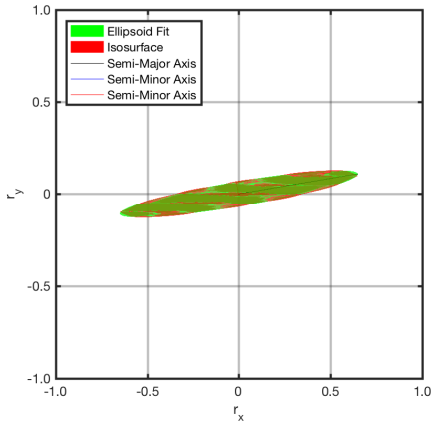

Figure 11. Isosurface and ellipsoid fit of the three-dimensional autocorrelation coefficient of Vorticity magnitude for a value of $Co_\omega = 0.3$ in the plane of shear for a rotation to shear rate ratio $f/S = +5$ at non-dimensional time $St = 10$.

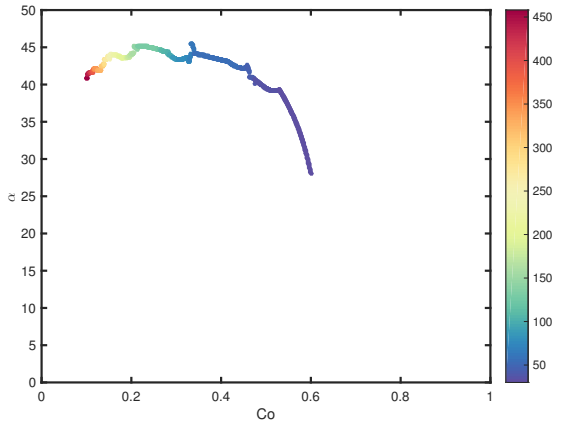

Figure 12. Dependence of the structure inclination angle α on the choice of the isovalue of the three-dimensional autocorrelation coefficient of vorticity magnitude Co_ω for a rotation to shear rate ratio $f/S = +0.5$ at non-dimensional time $St = 10$.

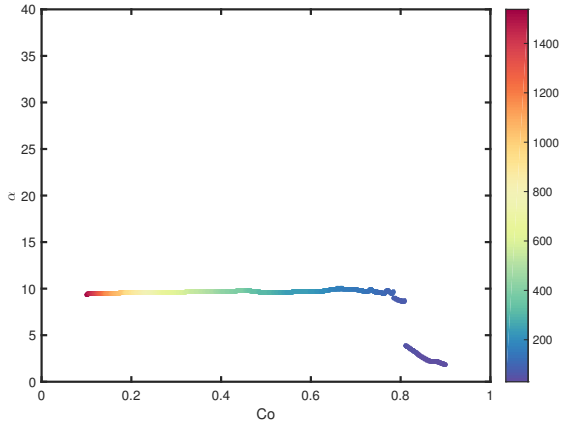

Figure 13. Dependence of the structure inclination angle α on the choice of the isovalue of the three-dimensional autocorrelation coefficient of vorticity magnitude Co_ω for a rotation to shear rate ratio $f/S = +5$ at non-dimensional time $St = 10$.

SUMMARY

Using the results of direct numerical simulations of homogeneous rotating and sheared turbulence, the orientation of vortical structures present in the flows is determined using isosurfaces of three-dimensional two-point autocorrelation coefficients of vorticity magnitude. The isosurfaces have an approximately ellipsoid shape and the inclination angle of the vortical structures are determined from the major axes of an ellipsoid least-squares fit to the isosurfaces.

The structure inclination angle α was observed to depend on the rotation to shear rate ratio f/S in the same fashion as the growth rate γ depends on f/S. An approximately linear relationship between the structure inclination angle and the growth rate of the turbulent kinetic energy was obtained.

Therefore, the structure of rotating and sheared homogeneous turbulence, as described by the structure inclination angle α, is directly related to the dynamics of the turbulent motion, as described by the growth rate γ of the turbulent kinetic energy. These results are in agreement with the findings by Jacobitz & Moreau (2016) for stably stratified turbulent shear flows.

ACKNOWLEDGMENTS

The authors acknowledge the support from the Shiley-Marcos School of Engineering and Information Technology Services at the University of San Diego. The computational work of this project was performed on the Saber1 cluster computer. JCA thanks the McNair Scholars Program for their ongoing support.

REFERENCES

Bakewell, H. P. & Lumley, J. L. 1967 Viscous sublayer and adjacent wall region in turbulent pipe flow. *Phys. Fluids* **10**, 1880–1889.

Bradshaw, P. 1969 The analogy between streamline curvature and buoyancy in turbulent shear flow. *J. Fluid Mech.* **36**, 177–191.

Brethouwer, G. 2005 The effect of rotation on rapidly sheared homogeneous turbulence and passive scalar transport. Linear theory and direct numerical simulation. *J. Fluid Mech.* **542**, 305–342.

Cambon, C., Benoit, J. P., Shao, L. & Jacquin, L. 1994 Stability analysis and large-eddy simulation of rotating turbulence. *J. Fluid Mech.* **278**, 175.

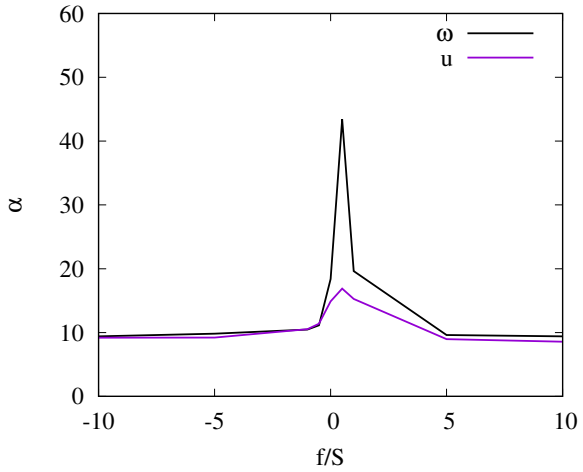

Figure 14. Dependence of the structure inclination angle α on the rotation to shear rate ratio f/S at non-dimensional time $St = 10$.

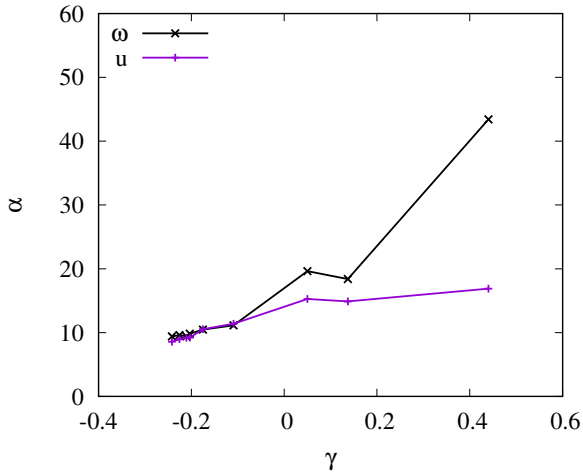

Figure 15. Dependence of the structure inclination angle α on the growth rate γ at non-dimensional time $St = 10$.

Clyne, J., Mininni, P., Norton, A. & Rast, M. 2007 Interactive desktop analysis of high resolution simulations: application to turbulent plume dynamics and current sheet formation. *New Journal of Physics* **9** (8), 301.

Dong, S., Lozano-Durán, A., Sekimoto, A. & Jiménez, J. 2017 Coherent structures in statistically stationary homogeneous shear turbulence. *J. Fluid Mech.* **816**, 167–208.

Jacobitz, F. G., Liechtenstein, L., Schneider, K. & Farge, M. 2008 On the structure and dynamics of sheared and rotating turbulence: Direct numerical simulation and wavelet-based coherent vortex extraction. *Phys. Fluids* **20**, 045103.

Jacobitz, F. G. & Moreau, A. F. 2016 Orientation of vortical structures in turbulent stratified shear flow. In *VIIIth International Symposium on Stratified Flows*, pp. 1–7. San Diego, CA.

Jacobitz, F. G., Schneider, K., Bos, W. J. T. & Farge, M. 2010 On the structure and dynamics of sheared and rotating turbulence: Anisotropy properties and geometrical scale-dependent statistics. *Phys. Fluids* **22**, 085101.

Jacobitz, F. G., Schneider, K., Bos, W. J. T. & Farge, M. 2016 Structure of sheared and rotating turbulence: Multiscale statistics of Lagrangian and Eulerian accelerations and passive scalar dynamics. *Phys. Rev. E* **93**, 013113.

Kassinos, S. C., Akylas, E. & Langer, C. A. 2007 Rapidly sheared homogeneous stratified turbulence in a rotating frame. *Phys. Fluids* **19**, 021701.

Kim, J. & Lim, J. 2000 A linear process in wall-bounded turbulent shear flows. *Phys. Fluids* **12**, 1885–1888.

Kline, S. J., Reynolds, W. C., Schraub, F. A. & Runstadler, P. W. 1967 The structure of turbulent boundary layers. *J. Fluid Mech.* **30**, 741–773.

Miesch, M. S. 2005 Large-scale dynamics of the convection zone and tachocline. *Living Reviews in Solar Physics* **2** (1), 1–139.

Rogallo, R. S. 1981 Numerical experiments in homogeneous turbulence. *NASA Report* **81315**.

Sagaut, P. & Cambon, C. 2008 *Homogeneous Turbulence Dynamics*. Cambridge, United Kingdom: Cambridge University Press.

Salhi, A 2002 Similarities between rotation and stratification effects on homogeneous shear flow. *Theoretical and Computational Fluid Dynamics* **15** (6), 339–358.

Salhi, A. & Cambon, C. 1997 An analysis of rotating shear flow using linear theory and DNS and LES results. *J. Fluid Mech.* **347**, 171.

Salhi, A., Jacobitz, F. G., Schneider, K. & Cambon, C. 2014 Nonlinear dynamics and anisotropic structure of rotating sheared turbulence. *Phys. Rev. E* **89**, 013020.

Theodorsen, T. 1952 Stabilization and destabilization of turbulent shear-flow in a rotating fluid. In *Second Midwestern Conference on Fluid Mechanics*, pp. 1–18. Ohio State University.

Tritton, D. J. 1992 Stabilization and destabilization of turbulent shear-flow in a rotating fluid. *J. Fluid Mech.* **241**, 503–523.

Wallace, J. M., Eckelman, H. & Brodkey, R. S. 1972 The wall region in turbulent shear flow. *J. Fluid Mech.* **54**, 39–48.